Electronic Supplementary Material (ESI) for Journal of Materials Chemistry A.

Electronic Supporting Information

A "turn-on" Cr^{3+} ion probe based on non-luminescent metal-organic framework–New strategy to prepare recovery probe

Experimental Procedures

Materials and physical measurements

All commercially available reagents and solvents were used as received without further purification. H_2L was synthesized according to reported methods.[1] Infrared spectra (IR) were recorded on Nicolet-20DXB spectrometer as KBr pellets in the range of 4000−400 cm^{-1}. The UV-visible absorption spectra were collected on a Hitachi U-3900 spectrophotometer. Thermogravimetric analyses (TGA) were performed under nitrogen atmosphere with a heating rate of 10 °C/min using a TA-Q50 thermogravimetric analyzer. Elemental analyses of C, H, and N were determined on a Vario EL Ⅲ elemental analyzer, while Cr was determined on a Perkinelmer OPTIMA 2000DV inductively coupled plasma emission spectrometer. Powder X-ray diffraction patterns (PXRD) data were collected on a Rigaku SmartLab 9KW X-ray diffractometer. Luminescent spectra were acquired at ambient temperature by using a Hitachi F-7000 fluorescence spectrophotometer. The fluorescenc lifetime were measured on a FLS1000 spectrophotometer (Edinburgh Instruments). A nanosecond pulsed diode laser with the excitation wavelength at 380 nm (EPL-380) was used for the measurements. Photoluminescence graphs were taken using a Canon camera (ixus 230 HS) under UV lamp irradiation.

Synthesis of $[Eu_2L_3(DMF)_3]\cdot 2DMF\cdot 5H_2O$ (1)

A mixture containing H_2L(0.11 mmol, 40 mg) and $Eu(NO_3)_3\cdot 6H_2O$(0.22 mmol, 98 mg) in DMF/H_2O(2mL/1mL) in a 20 mL scintillation vial was heated at 115 ºC for 2 d and then cooled to room temperature. The brown crystals were collected, washed with DMF and dried in air (42% yield). Element analysis (%) calcd for $C_{84}H_{90}Eu_2N_8O_{22}$: C, 54.02; H, 4.86; N, 5.99. Found: C,54.19; H,4.75; N, 5.68. IR (cm^{-1}): 3451(s), 3059(m), 1735(w), 1701(w), 1654(s), 1584(s), 1437(s), 1382(s), 782(m), 731(m), 707(w)。

Synthesis of $0.03Cr(NO_3)_3\cdot[Eu_2L_3(H_2O)(DMF)_2]\cdot 2DMF\cdot 10H_2O$ ($Cr(NO_3)_3$@1')

The compound was obtained by soaking the crystals of **1** in an aqueous solution of $Cr(NO_3)_3$ (0.01M) at room temperature for 24 h. The resulted crystals were collected by filtration, washed with H_2O and dried in air. Element analysis (%) calcd for $C_{81}H_{95}Cr_{0.03}Eu_2N_{7.09}O_{27.27}$: C, 50.94; H, 5.01; N, 5.20, Cr, 0.082. Found: C, 50.49; H, 5.05; N, 5.19; Cr, 0.083. IR (cm^{-1}): 3401(s), 1735(w), 1701(w), 1655(s), 1605(s), 1441(s), 1379(s), 785(m), 732(m), 667(w).

X-ray crystallographic study

Intensity data of single crystals was measured at 296(2) K on a Bruker SMART APEX II CCD area detector system. Data were corrected for absorption effects using the multi-scan technique (SADABS). The structure was solved by direct methods using SHELXS-2014 and was refined by full-matrix least squares methods using SHELXS-2014.[2] The hydrogen atoms were included in the structural model as fixed atoms "riding" on their respective carbon atoms using the idealized sp^2-hybridized geometry and C–H bond lengths of 0.95Å. Since the disordered DMF and H_2O solvent molecules could not be unambiguously modelled, the PLATON/SQUEEZE[3] program was utilized to calculate the solvent disorder area and remove

its contribution to the overall intensity data. The residual electron densities amounted to 130 e per formula, which roughly correspond to 2 DMF and 5 H_2O molecules for **1**, and 173 e per formula, which roughly correspond to 2 DMF and 10 H_2O molecules for $Cr(NO_3)_3$@**1'**. A summary of the most important crystal and structure refinement data is given in **Table S1**. Selected bond distances and angles are given in **Table S2** and **S3**. CCDC 2053671-2053672 contain the supplementary crystallographic data for this paper. The data can be obtained free of charge via www.ccdc.cam.ac.uk/conts/retrieving.html (or from the Cambridge Crystallographic Data Centre, 12 Union Road, Cambridge CB2 1EZ, UK; fax: (+44) 1223-336-033; or e-mail: deposit@ccdc.cam.ac.uk).

Luminescence sensing of ions in dispersions

Each sensing was repeated at least three times with consistent results. The excitation slit width and emission slit width in luminescent measurements were set to be 5 nm and 5 nm, respectively. Each time 1.5 mg finely-ground powders of **1** were dispersed in 3mL aqueous solution, stirred for 8 hours to form a stable emulsion for the luminescent studies. The titrations were carried out by gradually adding $Cr(NO_3)_3$ solutions (0.1M) into suspensions of **1**.

Hirshfeld surface analysis

The intermolecular interactions present in **1** and $Cr(NO_3)_3$@**1'** were investigated through Hirshfeld surface analysis by using CrystalExplorer 17.5 program.[4-6] By allocating the space in the crystal to the area where the electron density ratio (molecule) of the sum of spherical atoms in the molecule is equal to 0.5, the Hirshfeld surface of the molecule in the crystal is constructed. *de* and *di* are defined as the distance from the Hirshfeld surface to the nearest nucleus outside and inside the mean surface, respectively. *d*norm is the sum of *de* and *di* normalized by van der Waals radius (r^{vdw}). When the intermolecular contacts are closer, around and longer than the sum of their van der Waals radii, they are highlighted on the surface of Hirshfeld *d*norm in red, white and blue, respectively. A 2D fingerprint is generated by plotting the distribution of points derived from the Hirshfeld surface, which is used to summarize the interaction between molecules.[7] Each point on the 2D fingerprint map corresponds to a specific (*de*, *di*) coordinate, and the color of each point corresponds to the relative area of the surface with the (*de*, *di*). Points with small, medium, and large contribution to the surface contribution to the surface are colored from blue, through green to red.

Supporting Tables

Table S1. Crystallographic data for complex **1** and $Cr(NO_3)_3$@**1'**.

	1	$Cr(NO_3)_3$@**1'**
Formula	$C_{84}H_{90}Eu_2N_8O_{22}$	$C_{81}H_{95}Cr_{0.03}Eu_2N_{7.09}O_{27.27}$
Formula weight	1867.58	1909.72
Crystal system	Triclinic	Triclinic
Space group	P-1	P-1
a (Å)	16.0028(6)	16.1166(10)
b (Å)	16.4106(6)	16.1947(12)
c (Å)	17.9636(7)	17.9395(11)
α (°)	92.970(1)	93.188(2)
β (°)	110.088(2)	109.729(2)
γ (°)	110.910(2)	111.604(2)
V (Å^3)/ *Z*	4056.2(3)/2	4010.3(5) /2
D_{calcd} (g /cm^3)	1.336	1.305
μ(mm^{-1})	1.595	1.610
F(000)	1644	1584
θ range(°)	2.005 -25.000	2.786-25.000
Reflections collected / unique	68880/14160	59901 / 14074
R(int)	0.0243	0.0316
GOF on F^2	1.101	1.051
R_1[a], $I>2\sigma(I)$ (all)	0.0611 (0.0700)	0.0458 (0.0576)
wR_2[b], $I>2\sigma(I)$ (all)	0.1703 (0.1814)	0.1298 (0.1422)
Max/mean shift in final cycle	0.001/0.000	0.001/0.000

[a] $R=\sum(||F_o|-|F_c||)/\sum|F_o|$, [b] $Rw=\{\sum w[(F^2_o-F^2_c)]/\sum w[(F^2_o)^2]\}^{0.5}$, $w = [\sigma^2(F^2_o) + (aP)^2+bP]^{-1}$, where $P = (F^2_o +2 F^2_c)/3$.]. **1**, *a* = 0.1048, *b* = 26.4003. $Cr(NO_3)_3$@**1'**, *a* = 0.0865, *b* = 13.3181.

Table S2. Bond lengths (Å) and angles (°) for **1.**

Eu(1)-O(15)	2.374(6)	Eu(2)-O(13)	2.398(5)
Eu(1)-O(14)	2.378(7)	Eu(2)-O(5)	2.414(5)
Eu(1)-O(10)	2.382(4)	Eu(2)-O(7)#2	2.417(4)
Eu(1)-O(11)#1	2.427(5)	Eu(2)-O(4)#3	2.444(4)
Eu(1)-O(8)#2	2.435(5)	Eu(2)-O(1)	2.456(4)
Eu(1)-O(12)#1	2.456(5)	Eu(2)-O(3)#3	2.459(5)
Eu(1)-O(2)	2.486(5)	Eu(2)-O(9)	2.468(5)
Eu(1)-O(1)	2.511(4)	Eu(2)-O(6)	2.473(5)
Eu(1)-O(7)#2	2.704(5)	Eu(2)-O(10)	2.647(4)
O(15)-Eu(1)-O(14)	84.3(3)	O(13)-Eu(2)-O(5)	100.2(2)
O(15)-Eu(1)-O(10)	83.8(2)	O(13)-Eu(2)-O(7)#2	80.53(18)
O(14)-Eu(1)-O(10)	158.6(2)	O(5)-Eu(2)-O(7)#2	132.98(16)
O(15)-Eu(1)-O(11)#1	75.3(2)	O(13)-Eu(2)-O(4)#3	126.37(17)
O(14)-Eu(1)-O(11)#1	77.1(2)	O(5)-Eu(2)-O(4)#3	76.65(17)
O(10)-Eu(1)-O(11)#1	82.66(17)	O(7)#2-Eu(2)-O(4)#3	139.73(16)

O(15)-Eu(1)-O(8)#2	74.8(3)	O(13)-Eu(2)-O(1)	80.24(17)
O(14)-Eu(1)-O(8)#2	76.8(2)	O(5)-Eu(2)-O(1)	152.82(15)
O(10)-Eu(1)-O(8)#2	116.85(16)	O(7)#2-Eu(2)-O(1)	74.13(15)
O(11)#1-Eu(1)-O(8)#2	141.8(2)	O(4)#3-Eu(2)-O(1)	81.33(16)
O(15)-Eu(1)-O(12)#1	128.3(2)	O(13)-Eu(2)-O(3)#3	73.95(17)
O(14)-Eu(1)-O(12)#1	80.3(2)	O(5)-Eu(2)-O(3)#3	75.05(17)
O(10)-Eu(1)-O(12)#1	93.25(17)	O(7)#2-Eu(2)-O(3)#3	145.60(16)
O(11)#1-Eu(1)-O(12)#1	53.18(16)	O(4)#3-Eu(2)-O(3)#3	53.22(16)
O(8)#2-Eu(1)-O(12)#1	145.43(19)	O(1)-Eu(2)-O(3)#3	79.07(16)
O(15)-Eu(1)-O(2)	145.8(2)	O(13)-Eu(2)-O(9)	149.67(18)
O(14)-Eu(1)-O(2)	77.6(2)	O(5)-Eu(2)-O(9)	76.18(18)
O(10)-Eu(1)-O(2)	121.14(15)	O(7)#2-Eu(2)-O(9)	80.62(17)
O(11)#1-Eu(1)-O(2)	126.89(18)	O(4)#3-Eu(2)-O(9)	82.67(17)
O(8)#2-Eu(1)-O(2)	73.0(2)	O(1)-Eu(2)-O(9)	116.75(15)
O(12)#1-Eu(1)-O(2)	77.00(18)	O(3)#3-Eu(2)-O(9)	131.56(16)
O(15)-Eu(1)-O(1)	142.7(2)	O(13)-Eu(2)-O(6)	79.13(18)
O(14)-Eu(1)-O(1)	128.6(2)	O(5)-Eu(2)-O(6)	53.51(15)
O(10)-Eu(1)-O(1)	69.29(14)	O(7)#2-Eu(2)-O(6)	81.19(15)
O(11)#1-Eu(1)-O(1)	123.72(16)	O(4)#3-Eu(2)-O(6)	128.58(16)
O(8)#2-Eu(1)-O(1)	94.4(2)	O(1)-Eu(2)-O(6)	150.02(14)
O(12)#1-Eu(1)-O(1)	80.06(15)	O(3)#3-Eu(2)-O(6)	115.31(17)
O(2)-Eu(1)-O(1)	51.87(15)	O(9)-Eu(2)-O(6)	74.66(17)
O(15)-Eu(1)-O(7)#2	77.7(2)	O(13)-Eu(2)-O(10)	138.50(17)
O(14)-Eu(1)-O(7)#2	126.8(2)	O(5)-Eu(2)-O(10)	120.93(17)
O(10)-Eu(1)-O(7)#2	67.42(14)	O(7)#2-Eu(2)-O(10)	67.92(14)
O(11)#1-Eu(1)-O(7)#2	141.48(16)	O(4)#3-Eu(2)-O(10)	73.10(15)
O(8)#2-Eu(1)-O(7)#2	50.33(16)	O(1)-Eu(2)-O(10)	65.99(14)
O(12)#1-Eu(1)-O(7)#2	147.13(16)	O(3)#3-Eu(2)-O(10)	119.41(15)
O(2)-Eu(1)-O(7)#2	90.26(17)	O(9)-Eu(2)-O(10)	50.79(14)
O(1)-Eu(1)-O(7)#2	68.46(14)	O(6)-Eu(2)-O(10)	119.69(16)
Eu(2)-O(1)-Eu(1)	100.45(15)	Eu(1)-O(10)-Eu(2)	98.62(14)
Eu(2)#2-O(7)-Eu(1)#2	96.25(15)		

Symmetry transformations used to generate equivalent atoms:

#1: -x, -y, -z+1; #2: -x+1, -y+1, -z+1; #3: -x, -y+1, -z+1.

Table S3. Selected bond lengths (Å) and angles (°) for $Cr(NO_3)_3$@**1'**.

Eu(1)-O(13)	2.377(4)	Eu(2)-O(14)	2.343(5)
Eu(1)-O(5)	2.408(4)	Eu(2)-O(10)	2.382(4)
Eu(1)-O(7)#1	2.439(4)	Eu(2)-O(15)	2.411(5)
Eu(1)-O(1)	2.440(4)	Eu(2)-O(11)#3	2.428(4)
Eu(1)-O(4)#2	2.454(4)	Eu(2)-O(8)#1	2.430(4)
Eu(1)-O(3)#2	2.458(4)	Eu(2)-O(12)#3	2.450(4)
Eu(1)-O(9)	2.466(4)	Eu(2)-O(2)	2.476(4)
Eu(1)-O(6)	2.487(4)	Eu(2)-O(1)	2.516(4)
Eu(1)-O(10)	2.611(4)	Eu(2)-O(7)#1	2.645(4)
O(13)-Eu(1)-O(5)	100.48(17)	O(14)-Eu(2)-O(10)	157.31(18)

O(13)-Eu(1)-O(7)#1	81.45(15)	O(14)-Eu(2)-O(15)	85.8(2)
O(5)-Eu(1)-O(7)#1	134.20(13)	O(10)-Eu(2)-O(15)	80.68(16)
O(13)-Eu(1)-O(1)	81.82(14)	O(14)-Eu(2)-O(11)#3	75.62(18)
O(5)-Eu(1)-O(1)	152.47(13)	O(10)-Eu(2)-O(11)#3	83.16(14)
O(7)#1-Eu(1)-O(1)	73.32(13)	O(15)-Eu(2)-O(11)#3	74.12(16)
O(13)-Eu(1)-O(4)#2	126.63(14)	O(14)-Eu(2)-O(8)#1	76.22(17)
O(5)-Eu(1)-O(4)#2	76.87(13)	O(10)-Eu(2)-O(8)#1	117.16(13)
O(7)#1-Eu(1)-O(4)#2	137.68(13)	O(15)-Eu(2)-O(8)#1	75.20(19)
O(1)-Eu(1)-O(4)#2	79.87(13)	O(11)#3-Eu(2)-O(8)#1	139.39(17)
O(13)-Eu(1)-O(3)#2	74.22(14)	O(14)-Eu(2)-O(12)#3	80.01(18)
O(5)-Eu(1)-O(3)#2	75.35(14)	O(10)-Eu(2)-O(12)#3	93.75(14)
O(7)#1-Eu(1)-O(3)#2	145.34(13)	O(15)-Eu(2)-O(12)#3	127.25(16)
O(1)-Eu(1)-O(3)#2	79.02(13)	O(11)#3-Eu(2)-O(12)#3	53.17(13)
O(4)#2-Eu(1)-O(3)#2	53.25(12)	O(8)#1-Eu(2)-O(12)#3	145.82(15)
O(13)-Eu(1)-O(9)	147.44(16)	O(14)-Eu(2)-O(2)	79.41(19)
O(5)-Eu(1)-O(9)	74.88(15)	O(10)-Eu(2)-O(2)	120.81(13)
O(7)#1-Eu(1)-O(9)	79.76(14)	O(15)-Eu(2)-O(2)	148.42(17)
O(1)-Eu(1)-O(9)	117.32(13)	O(11)#3-Eu(2)-O(2)	127.46(14)
O(4)#2-Eu(1)-O(9)	84.37(14)	O(8)#1-Eu(2)-O(2)	74.24(17)
O(3)#2-Eu(1)-O(9)	132.53(14)	O(12)#3-Eu(2)-O(2)	77.54(14)
O(13)-Eu(1)-O(6)	78.50(15)	O(14)-Eu(2)-O(1)	130.01(19)
O(5)-Eu(1)-O(6)	53.22(12)	O(10)-Eu(2)-O(1)	68.85(12)
O(7)#1-Eu(1)-O(6)	83.24(13)	O(15)-Eu(2)-O(1)	141.61(15)
O(1)-Eu(1)-O(6)	151.32(12)	O(11)#3-Eu(2)-O(1)	122.50(14)
O(4)#2-Eu(1)-O(6)	128.74(13)	O(8)#1-Eu(2)-O(1)	98.04(16)
O(3)#2-Eu(1)-O(6)	114.79(14)	O(12)#3-Eu(2)-O(1)	78.93(13)
O(9)-Eu(1)-O(6)	73.09(14)	O(2)-Eu(2)-O(1)	51.97(12)
O(13)-Eu(1)-O(10)	140.54(14)	O(14)-Eu(2)-O(7)#1	127.05(16)
O(5)-Eu(1)-O(10)	118.57(14)	O(10)-Eu(2)-O(7)#1	67.97(12)
O(7)#1-Eu(1)-O(10)	67.76(12)	O(15)-Eu(2)-O(7)#1	78.76(15)
O(1)-Eu(1)-O(10)	66.46(11)	O(11)#3-Eu(2)-O(7)#1	143.09(13)
O(4)#2-Eu(1)-O(10)	71.73(12)	O(8)#1-Eu(2)-O(7)#1	50.92(13)
O(3)#2-Eu(1)-O(10)	119.04(12)	O(12)#3-Eu(2)-O(7)#1	146.69(13)
O(9)-Eu(1)-O(10)	51.00(12)	O(2)-Eu(2)-O(7)#1	88.10(14)
O(6)-Eu(1)-O(10)	119.60(13)	O(1)-Eu(2)-O(7)#1	68.66(12)
Eu(1)-O(1)-Eu(2)	100.01(12)	Eu(2)-O(10)-Eu(1)	98.91(12)
Eu(1)#1-O(7)-Eu(2)#1	96.55(12)		

Symmetry transformations used to generate equivalent atoms:

#1 -x+2, -y+1, -z+1; #2 -x+1, -y+1, -z+1; #3 -x+1, -y, -z+1

Table S4. The LOD calculation of **1**.

K =1.8×10^7	The slope of the calibration curve (see Fig. 5 in the text)
σ=*0.451*	The standard deviation of the blank solution
LOD=*3*σ/*K* =3×0.451/1.8×10^7=7.52×10^{-8} M	

Table S5. A comparison of LODs toward Cr^{3+} ion for some probes.

Compound	method	LOD	Sensing type	Working solvent	Reference
$\{[Zn_2(tpeb)_2(2,3\text{-}ndc)_2]\cdot H_2O\}_n$	fluorescence	1.69×10^{-8} M	Turn off	H_2O	8
$\{[Eu(HL_1)(H_2O)_3]\cdot H_2O\}_n$	fluorescence	0.41×10^{-6} M	Turn off	H_2O	9
$\{[Zn_2(\mu_3\text{-}OH)(cpta)(4,4'\text{-}bipy)]\cdot H_2O\}_n$	fluorescence	5.55×10^{-6} M	Turn off	H_2O	10
$[Eu_2(tpbpc)_4\cdot CO_3\cdot H_2O]\cdot DMF$	fluorescence	7.00×10^{-5} M	Turn off	H_2O	11
$Zn_3(bpdc)_2(pdc)(DMF)\cdot 6DMF$	fluorescence	2.51×10^{-5} M	Turn off	H_2O	12
$[Eu(L_2)(HCOO)(H_2O)]_n$	fluorescence	1.51×10^{-6} M	Turn off	H_2O	13
$[Zn(L_3)(H_2O)]\cdot H_2O$	fluorescence	2.44×10^{-6} M	Turn off	H_2O	14
$[Zn_2(TPOM)(NH_2\text{-}BDC)_2]\cdot 4H_2O$	fluorescence	1.88×10^{-6} M	Turn on	DMF	15
$\{[Cd_2(adc)_2(4\text{-}nvp)_6]\cdot MeOH\cdot H_2O\}_n$	fluorescence	0.31×10^{-6} M	Turn on	CH_3CN /H_2O	16
$[Zn\ (tbda)]_n$	fluorescence	0.18×10^{-3} M	Turn on	H_2O	17
$[Cd_4(NDC)_3(4\text{-}Hptz)_2(H_2O)_2]\cdot H_2O$	fluorescence	0.16×10^{-6} M	Turn on	H_2O	18
YF_3: Eu^{3+} nanoparticles	fluorescence	1.88×10^{-6}M	Turn off	H_2O	19
Rh6G-AuNPs	fluorescence	9.28×10^{-6}M	Turn on	H_2O	20
Eu^{3+}(5%)-Gd_2O_3 nanoparticles	fluorescence	4.14×10^{-5}M	Turn off	H_2O	21
PVP@Gd_2O_3:Eu^{3+} NPs	fluorescence	2.10×10^{-6}M	Turn off	H_2O	22
Cu NPs	fluorescence	3.00×10^{-8}M	Turn off	MOPS buffer	23
AO/AuNP	fluorescence	2.00×10^{-8}M	Turn on	H_2O	24
(PIN/CdS) nanocomposite	fluorescence	4.70×10^{-7}M	Turn on	PBS buffer	25
RB-PEG-PAA-MNPs	fluorescence	1.31×10^{-7}M	Turn on	MeOH/H_2O	26
rhodamine-benzothiazole	fluorescence	0.36×10^{-7}M	ratiometric	MeOH/H_2O	27
2-((9H-fluoren-2-ylimino)methyl)phenol	fluorescence	2.50×10^{-7}M	Turn on	CH_3CN	28
bissalamo-coumarin	fluorescence	4.87×10^{-7}M	Turn off	ethanol	29
rhodamine 6G–en	fluorescence	0.31×10^{-6}M	Turn on	methanol/H_2O	30
orange emission carbon dots	fluorescence	0.38×10^{-6} M	Turn off	Tris-HCl buffer	31
S/N-CQDs	fluorescence	6.00×10^{-6} M	Turn off	H_2O	32
$[Eu_2L_3(DMF)_3]\cdot 2DMF\cdot 5H_2O$	fluorescence	7.52×10^{-8} M	Recovery	H_2O	This work

Table S6. Assay results for Cr^{3+} detection in real samples (n = 3).

Sample	Cr^{3+}found (μM)	added Cr^{3+} (μM)	found Cr^{3+} (μM)	Recovery (%)	RSD (%)
tap water	NOT found	100	95.88	95.88%	1.61%
		200	196.87	98.43%	1.19%

		300	295.79	98.60%	1.02%
sea water	NOT found	100	97.81	97.81%	1.64%
		200	196.18	98.09%	1.11%
		300	295.84	98.61%	1.02%

Supporting Figures

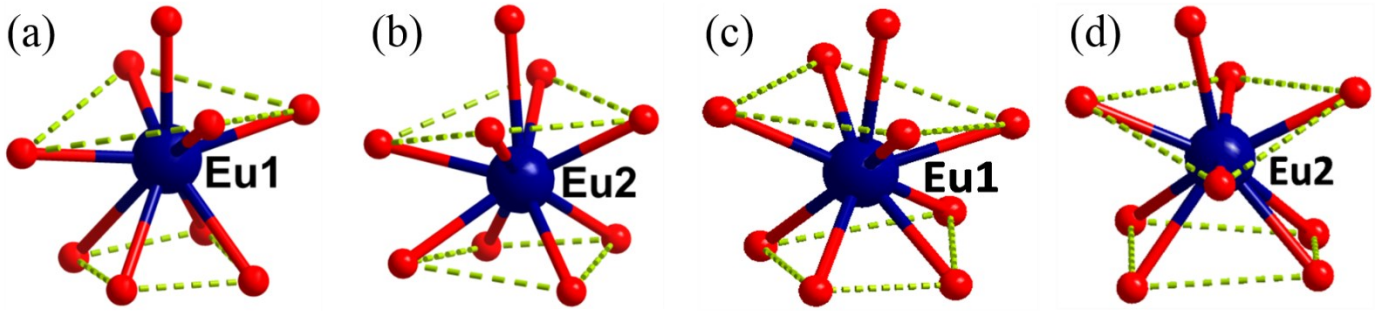

Figure. S1 Coordination polyhedra of Eu1 (a) and Eu2 (b) in **1**. Coordination polyhedra of Eu1 (c) and Eu2 (d) in $Cr(NO_3)_3$@**1'.**

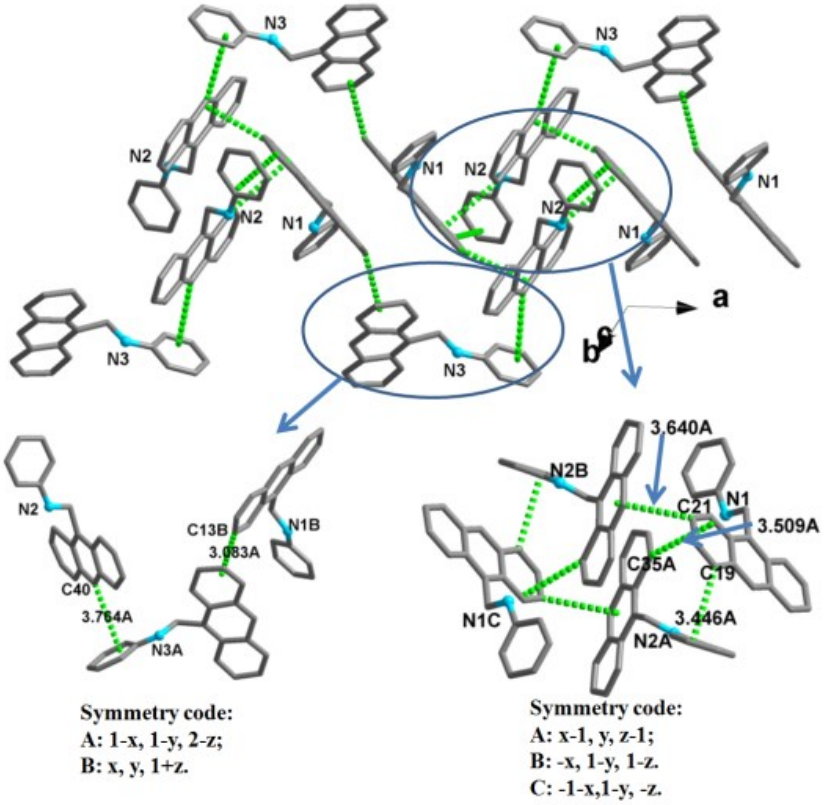

Figure. S2 The π–π interactions (represented as green dotted line) in the packing structure of **1**.

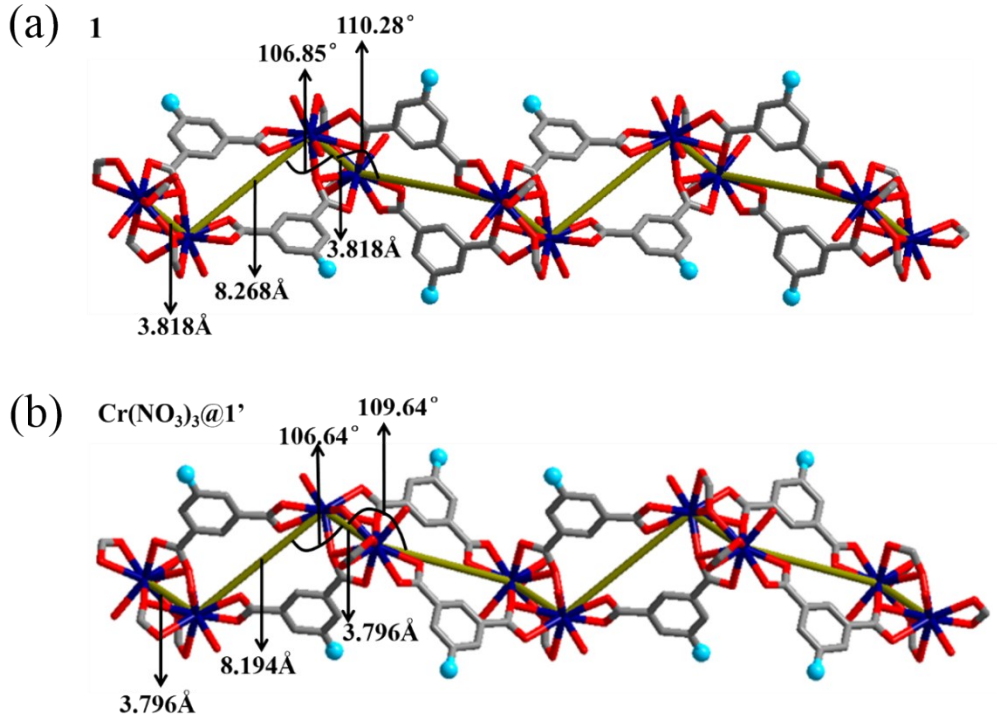

Figure. S3 A comparsion of the skeleton of the 2D net in **1** (a) and $Cr(NO_3)_3$@**1'** (b) to shown that the introduction of Cr^{3+} ions cause deformation of the framework. Both of them are viewed along the *c* direction. The 9-anthrylmethyl groups are omitted for clarity.

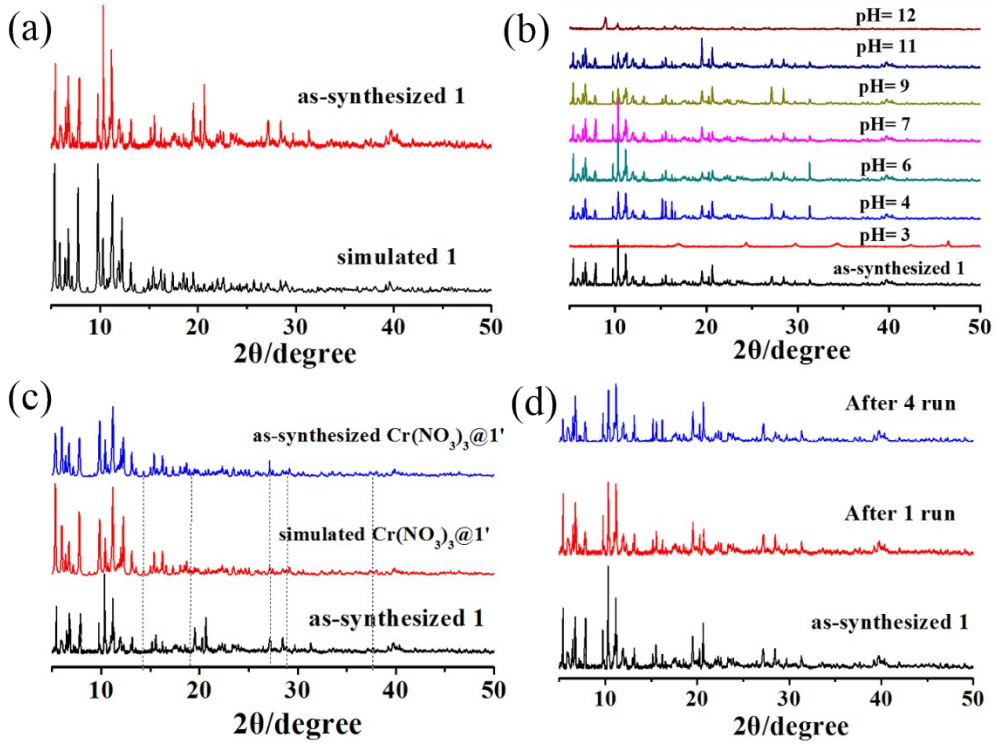

Figure. S4 (a) PXRD patterns of simulated **1** (black) and as-synthesized **1** (red). (b) A comparsion of PXRD patterns of as-synthesized **1** and the samples of **1** after being soaked in aqueous solutions with pH in the range of 3-12 for 24 hrs. (c) PXRD patterns of as-synthesized **1** (black), simulated $Cr(NO_3)_3$@**1'** (red) and as-synthesized $Cr(NO_3)_3$@**1'** (blue). (d) The results of PXRD of **1** before and after four cycles of the detection of Cr^{3+} ion.

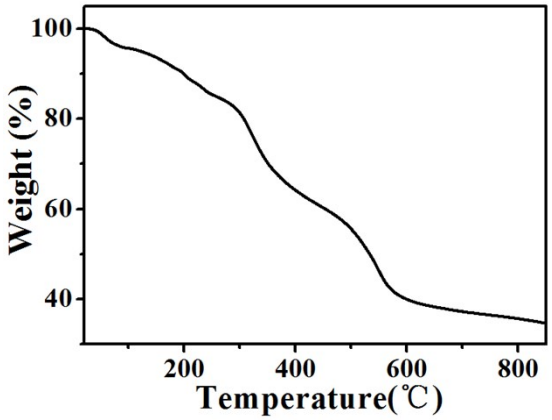

Figure. S5 The TGA curve of **1** in a N_2 flow from 25 °C to 850 °C.

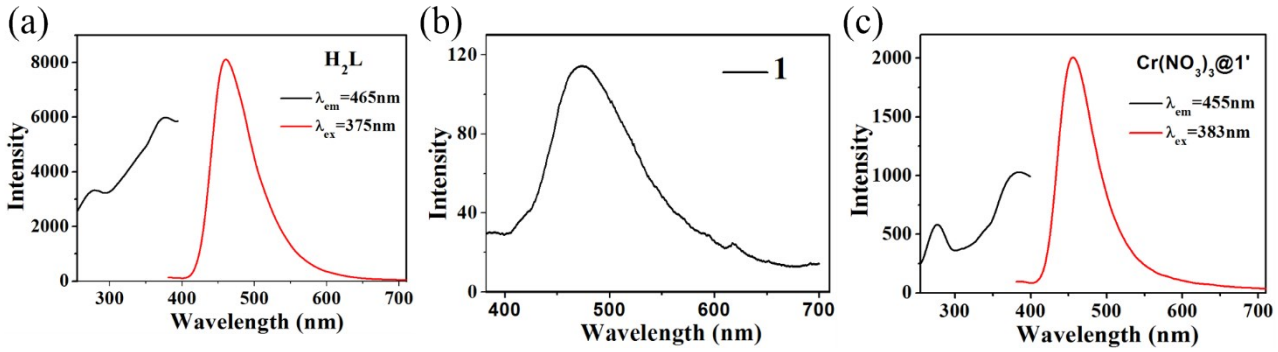

Figure. S6 (a) Solid state excitation and emission spectra of free **H_2L** ligand. (b) and (c) are the solid-state photoluminescence spectra of **1** and $Cr(NO_3)_3$@**1'**at room temperature.

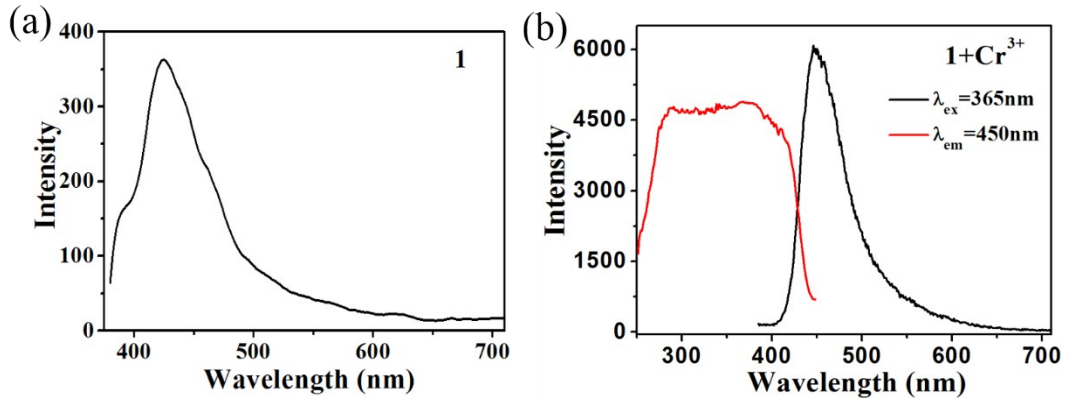

Figure. S7 (a) Emission spectrum of suspension of **1** in H_2O. (b) The excitation and emission spectra of suspension of **1** dispersed in 1.0×10^{-3} M Cr^{3+} solution.

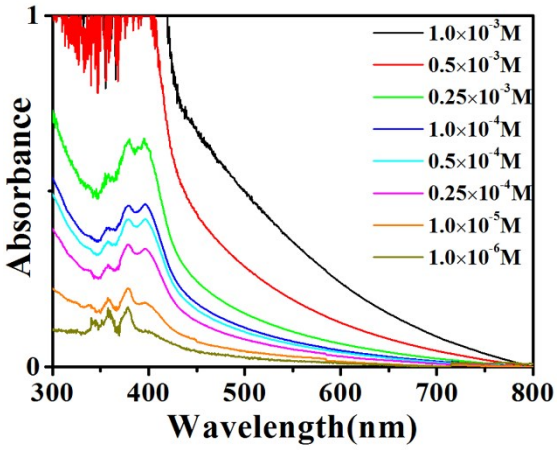

Figure. S8 UV-Vis spectra of different concentrations of H_2L in H_2O.

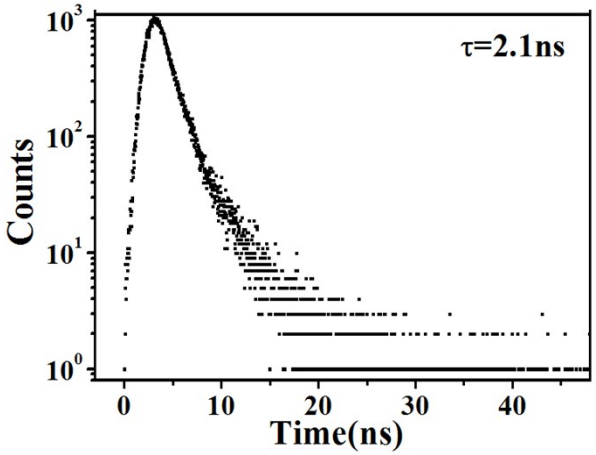

Figure. S9 Luminescence decay curve of $Cr(NO_3)_3$@**1'** (λ_{ex}=380 nm).

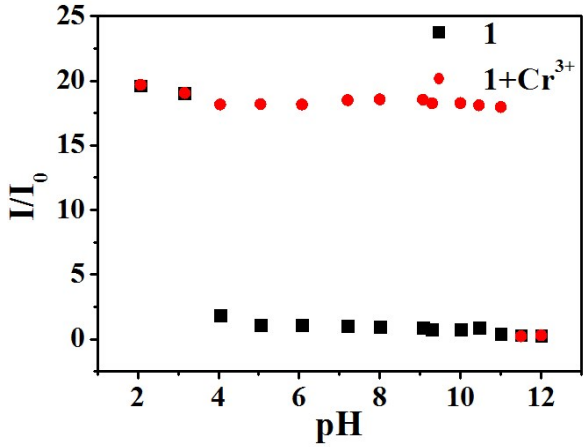

Figure. S10 Luminescence response at 425 nm for suspension of **1** (black square) and at 450 nm for suspension of **1** dispersed in 1.0×10^{-3} M Cr^{3+} solution (red circle) as a function of pH in H_2O. The pH was adjusted by 1 M aqueous solutions of HCl or NaOH. λ_{ex}=365 nm.

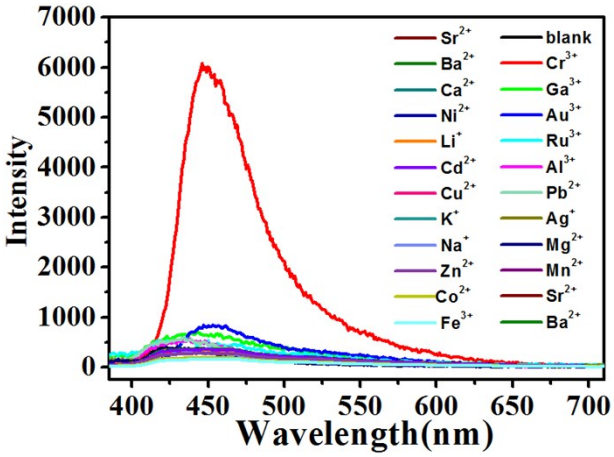

Figure. S11 Emission spectra (λ_{ex}=365 nm) of suspension of **1** dispersed in 1.0×10^{-3} M aqueous solution of different metal ions.

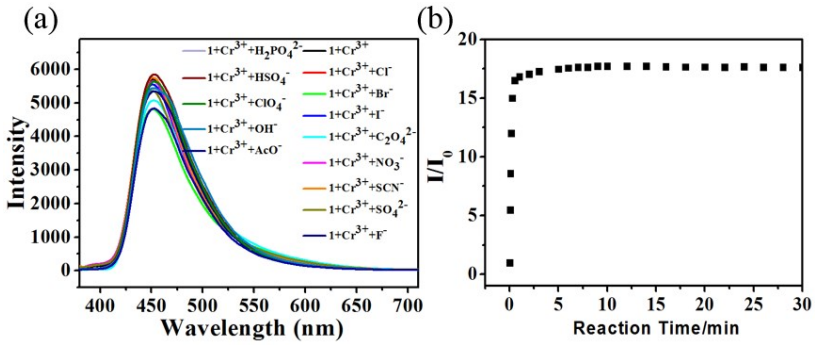

Figure. S12 (a) Luminescence response of suspension of **1** dispersed in 1.0×10^{-3} M Cr^{3+} solution and 1.0×10^{-3} M of various potassium salts in aqueous solution (λ_{ex}=365 nm). (b) Luminescence intensity of suspension of **1** as a function of immersion time when 1.0×10^{-3} M Cr^{3+} aqueous solution was added.

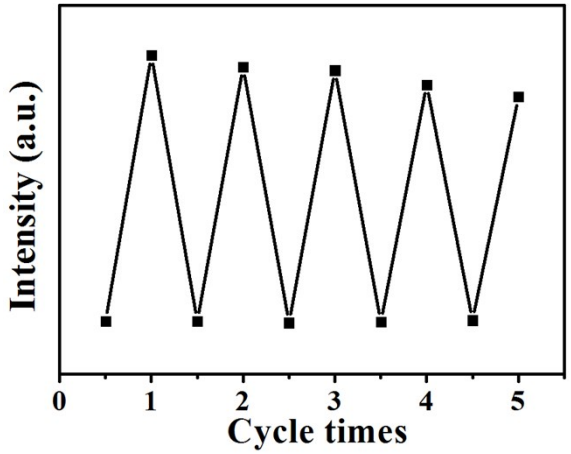

Figure. S13 The results of emission intensities of suspension of **1** before and after the detection of Cr^{3+} ion for five continuous cycles.

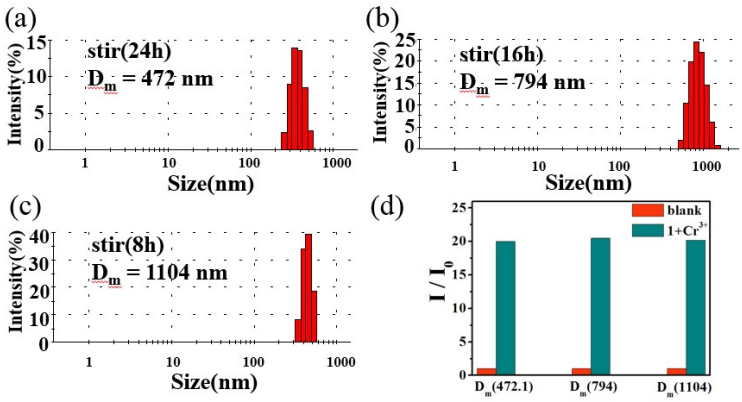

Figure. S14 Dynamic light scattering (DLS) of probe 1 at different stirring times(a: stir 8h,b: stir 16h,c: stir 24h). (d) Luminescence response of suspension of **1** with different particle sizes dispersed in 1.0×10^{-3} M Cr^{3+} solution**.**

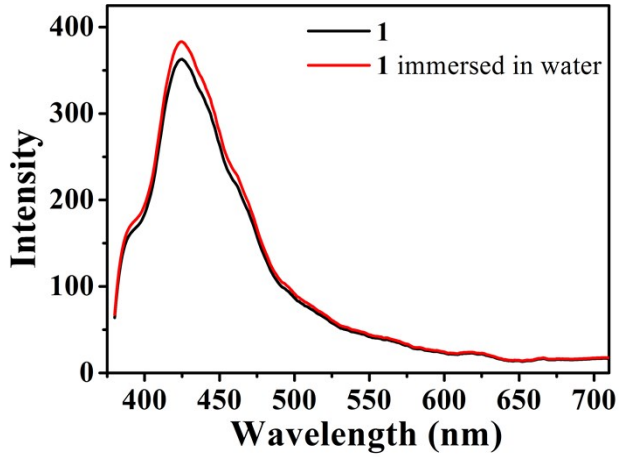

Figure. S15 A comparsion of emission spectra of suspensions of freshly prepared **1** in aqueous solution and **1** after being immersed in water for 2 months.

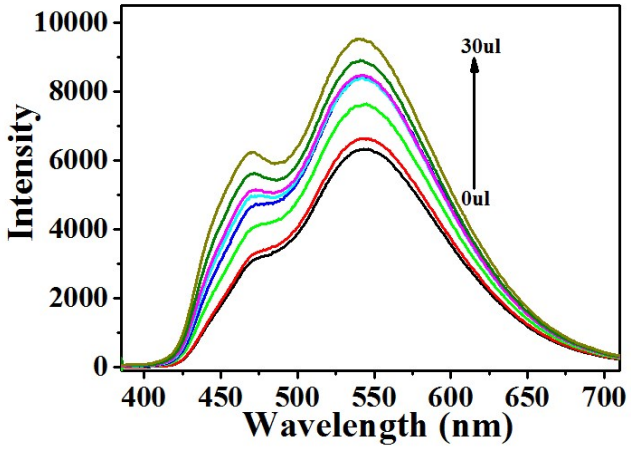

Figure. S16 The emission spectra of H_2L (1.34×10^{-3}M) in H_2O upon an incremental addition of 0.1 M Cr^{3+} solution.

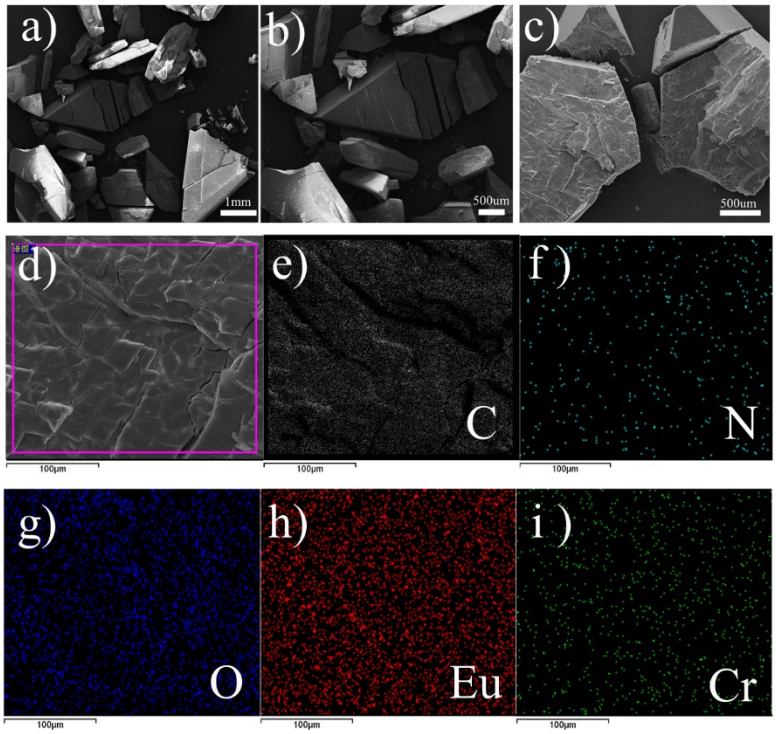

Figure. 17 SEM images of **1** (a)**,** $Cr(NO_3)_3$@**1'** (b)**.** (c) A view of the cross sections of $Cr(NO_3)_3$@**1'**. (d) Original image of TEM elemental mapping of $Cr(NO_3)_3$@**1'**. (e-i) TEM elemental mapping of C (gray), N (sky blue), O(blue), Eu (red) and Cr(green) of $Cr(NO_3)_3$@**1'**, respectively.

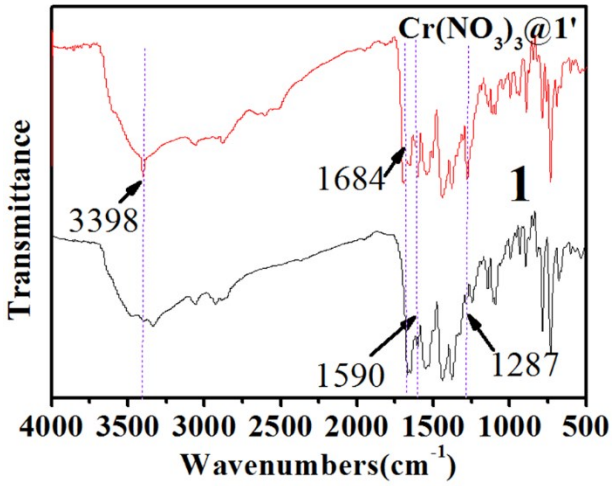

Figure. S18 A comparsion of IR spectra of **1** and $Cr(NO_3)_3$@**1'.**

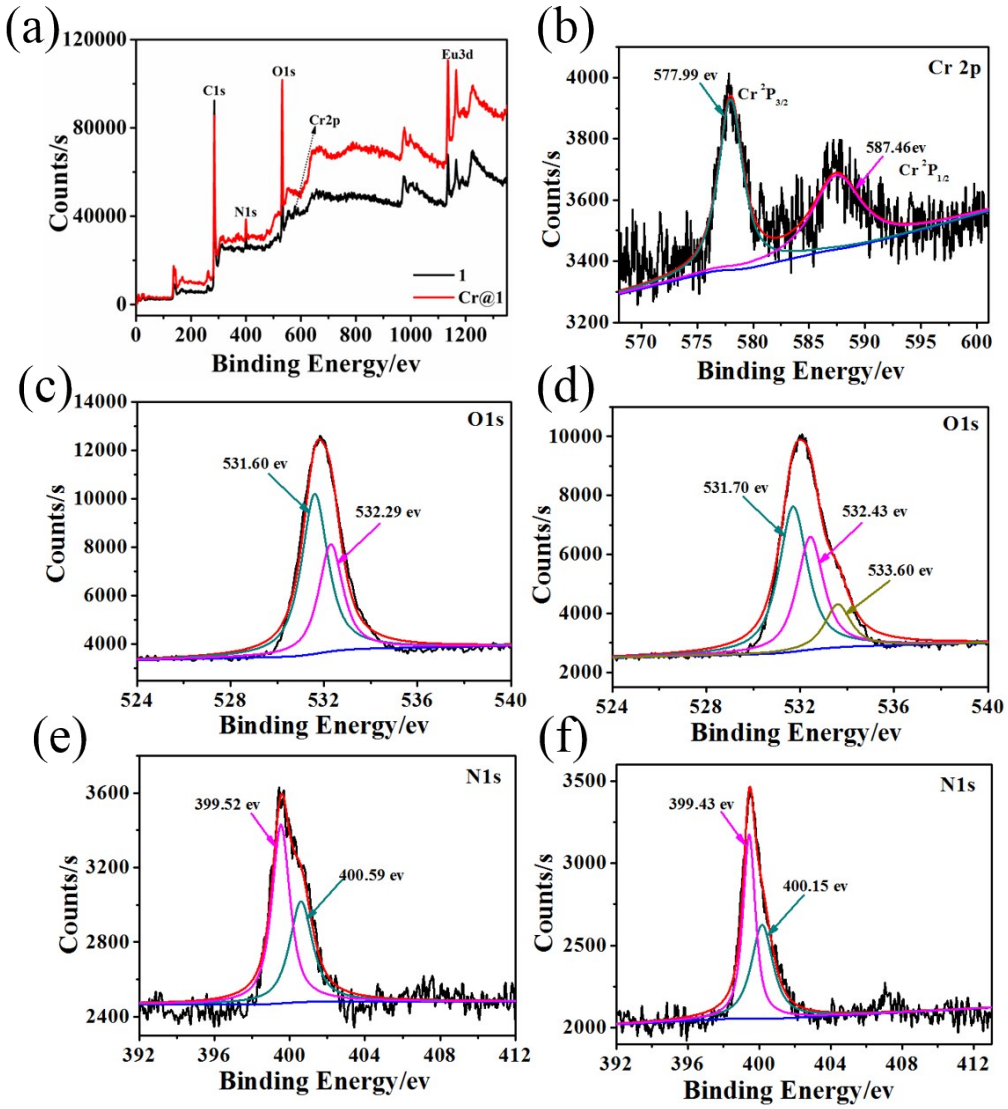

Figure. S19 A comparsion of XPS spectra of **1** and $Cr(NO_3)_3$@**1'.** (a) Overall spectra of **1** and $Cr(NO_3)_3$@**1'**. (b) Cr core-level spectrum of $Cr(NO_3)_3$@**1'.** (c) O1s core-level spectrum of **1**; (d) O1s core-level spectrum of $Cr(NO_3)_3$@**1'**; (e) N 1s core-level spectrum of **1**; (f) N 1s core-level spectrum of $Cr(NO_3)_3$@**1'**.

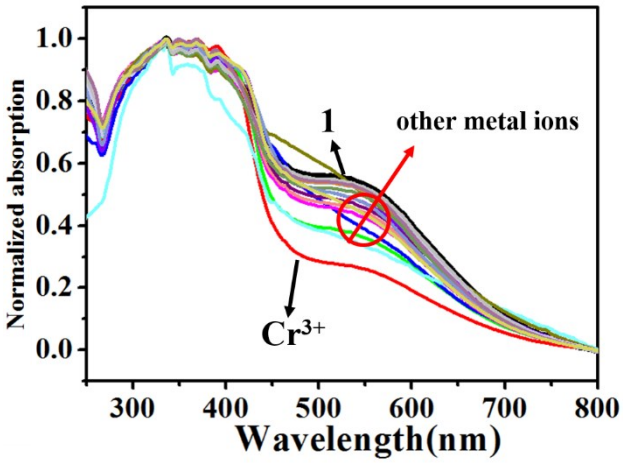

Figure. S20 The UV-Vis diffuse reflectance spectra o**f 1**(black line)**, 1** soaked in Cr^{3+}(red line) and other metal ions(Al^{3+}, Pb^{2+}, Mg^{2+}, Mn^{2+}, Sr^{2+}, Ba^{2+}, Ca^{2+}, Ni^{2+}, Li^{+}, Cd^{2+}, Cu^{2+}, K^{+}, Na^{+}, Zn^{2+}, Co^{2+}, Fe^{3+}, Au^{3+}, Ga^{3+}, Ru^{3+}, Ag^{+}).

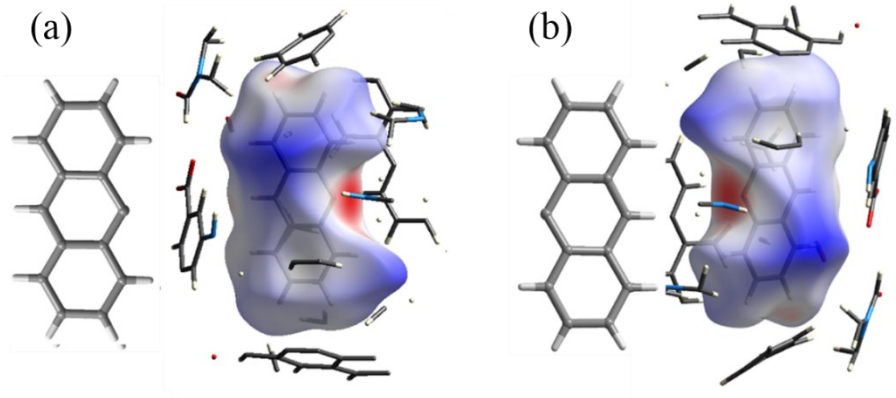

Figure. S21 The Hirshfeld d_{norm} surfaces of the anthracene ring in **1** (a) and $Cr(NO_3)_3$@**1'** (b).

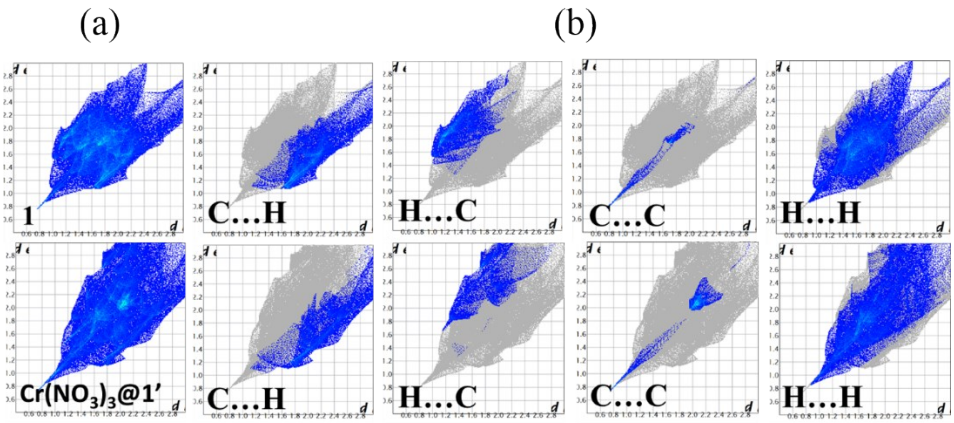

Figure. S22 The fingerprint plots of intermolecular interactions for anthracene ring in **1** and $Cr(NO_3)_3$@**1'.** (a) is the general graph, (b) is the sub-graph of various weak interaction.

Supporting references

1. R. Singh, J. Mrozinski and P. K. Bharadwaj, *Cryst. Growth Des.*, 2014, **14**, 3623-3633.
2. G. M. Sheldrick, *Acta Cryst.*, 2015, **71**, 3-8.
3. A. L. P. Spek, Multipurpose Crystallographic Tool, Utrecht University, Utrecht, The Netherlands,, 2008.
4. M. A. Spackman and D. Jayatilaka, *CrystEngComm,* , 2009, **11**, 19-32.
5. R. Arulraj, S. Sivakumar, K. Rajkumar, J. P. Jasinski, M. Kaur and A. Thiruvalluvar, *J. Chem. Crystallogr.*, 2019, **50**, 41-51.
6. M. J. Turner MJ, Wolff SK, Grimwood DJ, Spackman, J. D. PR, Spackman MA (2017) CrystalExplorer 17.5, and h. h. n. University of Western Australia.
7. M. A. Spackman and J. J. McKinnon, *CrystEngComm.*, 2002, **4**, 378-392.
8. T. Y. Gu, M. Dai, D. J. Young, Z. G. Ren and J. P. Lang, *Inorg. Chem.*, 2017, **56**, 4669-4679.
9. H. Wang, J. Qin, C. Huang, Y. Han, W. Xu and H. Hou, *Dalton Trans.*, 2016, **45**, 12710-12716.
10. H. Jin, J. Xu, L. Zhang, B. Ma, X. Shi, Y. Fan and L. Wang, *J. Solid State Chem.*, 2018, **268**, 168-174.
11. J. Liu, G. Ji, J. Xiao and Z. Liu, *Inorg. Chem.*, 2017, **56**, 4197-4205.
12. X. Meng, M. J. Wei, H. N. Wang, H. Y. Zang and Z. Y. Zhou, *Dalton Trans.*, 2018, **47**, 1383-1387.
13. Z. Sun, M. Yang, Y. Ma and L. Li, *Cryst. Growth Des.*, 2017, **17**, 4326-4335.

14. X.-Y. Guo, F. Zhao, J.-J. Liu, Z.-L. Liu and Y.-Q. Wang, *J. Mater. Chem. A*, 2017, **5**, 20035-20043.
15. R. Lv, J. Wang, Y. Zhang, H. Li, L. Yang, S. Liao, W. Gu and X. Liu, *J. Mater. Chem. A*, 2016, **4**, 15494-15500.
16. B. Dutta, R. Jana, A. K. Bhanja, P. P. Ray, C. Sinha and M. H. Mir, *Inorg. Chem.*, 2019, **58**, 2686-2694.
17. X. Liang, Y. Jia, Z. Zhan and M. Hu, *Appl. Organomet. Chem.*, 2019, **33**.
18. H. Li, D. Li, B. Qin, W. Li, H. Zheng, X. Zhang and J. Zhang, *Dyes Pigm.*, 2020, **178**.
19. L. Li, F.-F. Chen, J. Pan, S. Zhong, L. Li and Y. Yu, *J. Lumin.*, 2020, **226**.
20. N. Manjubaashini, T. Daniel Thangadurai, G. Bharathi and D. Nataraj, *J. Lumin.*, 2018, **202**, 282-288.
21. S. Chaudhary, S. Kumar, A. Umar, J. Singh, M. Rawat and S. K. Mehta, *Sensors and Actuators B: Chemical*, 2017, **243**, 579-588.
22. N. Vashistha, A. Chandra and M. Singh, *New J. Chem.*, 2020, **44**, 14211-14227.
23. C. Chen, F. Geng, Y. Wang, H. Yu, L. Li, S. Yang, J. Liu and W. Huang, *Talanta*, 2019, **205**, 120132.
24. L. Wang, J. Liu, Z. Zhou, M. Xu and B. Wang, *Analytical Methods*, 2017, **9**, 1786-1791.
25. M. Faraz, A. Abbasi, F. K. Naqvi, N. Khare, R. Prasad, I. Barman and R. Pandey, *Sensors and Actuators B: Chemical*, 2018, **269**, 195-202.
26. J. Wu, W. Jiang, S. Xu, Y. Wang and R. Tian, *Sensors and Actuators B: Chemical*, 2015, **211**, 33-41.
27. Y. Yang, Y. Feng, Y.-Z. Wang, F.-Z. Qiu, X.-L. Tang, G.-L. Zhang and W.-S. Liu, *Sensors and Actuators B: Chemical*, 2017, **253**, 1055-1062.
28. M. Tajbakhsh, G. B. Chalmardi, A. Bekhradnia, R. Hosseinzadeh, N. Hasani and M. A. Amiri, *Spectrochim Acta A Mol Biomol Spectrosc*, 2018, **189**, 22-31.
29. P. Zhang, X. Xu, Y.-F. Cui, X.-H. Wei, S.-J. memg and Y.-X. Sun, *Journal of Photochemistry and Photobiology A: Chemistry*, 2021, **408**.
30. R. Alam, R. Bhowmick, A. S. M. Islam, A. katarkar, K. Chaudhuri and M. Ali, *New J. Chem.*, 2017, **41**, 8359-8369.
31. J. Si, H. Wang, B. Wu, G. Wang, J. Yang, Z. Huo, T. Tian, X. Zhao and S. Han, *Micro & Nano Letters*, 2020, **16**, 58-63.
32. C. Wang, J. Xu, H. Li and W. Zhao, *Luminescence*, 2020, **35**, 1373-1383.